*Acc. Chem. Res.* **2006,** *39,* 558−566

# Correlating Structure with Function in Bacterial Multicomponent Monooxygenases and Related Diiron Proteins

MATTHEW H. SAZINSKY AND STEPHEN J. LIPPARD*

*Department of Chemistry, Massachusetts Institute of Technology, Cambridge, Massachusetts 02139*

Received February 28, 2006

**ABSTRACT**

Bacterial multicomponent monooxygenases (BMMs) catalyze the $O_2$-dependent hydroxylation of hydrocarbons at a carboxylate-bridged diiron center similar to those that occur in a variety of dimetallic oxygen-utilizing enzymes. BMMs have found numerous biodegradation and biocatalytic applications. Recent investigations have begun to reveal how BMMs perform their C−H bond activation chemistry and why these enzymes may be mechanistically different from other related diiron proteins. The structures of the BMM component proteins and of complexes between them provide insights into the tuning of the dinuclear iron center and the enzyme mechanism. Selected findings are compared and contrasted with the properties of other carboxylate-bridged diiron proteins, revealing common structural and functional themes.

## Introduction

Nature has evolved carboxylate-bridged diiron centers in proteins to perform a variety of functions. Included among the functions of proteins in this superfamily are iron storage in ferritin, $O_2$ transport in hemerythrin, radical generation in ribonucleotide reductase (RNR-R2), peroxide scavenging in rubrerythrin, hydrocarbon desaturation in stearoyl-acyl carrier protein $\Delta^9$ desaturase, and hydrocarbon oxidation in multicomponent monooxygenases.[1,2] In all of these proteins, the dimetallic center is housed within a four-helix bundle, a preferred biological scaffold for binding and activating $O_2$. In the majority of those systems in which dioxygen activation chemistry is performed, four of the iron-coordinating ligands are provided by two E(D/H)XXH motifs. The different functions and activities of these enzymes derive from the surrounding protein environment, which evolved to control the primary and secondary coordination spheres of the dimetallic center, introduce active-site pockets, afford substrate access and product egress channels, and create electron-transfer (ET) pathways.

The bacterial multicomponent monooxygenase (BMM) family of enzymes includes methane/butane monooxygenases (sMMOs), four-component alkene/aromatic monooxygenases (TMOs), phenol hydroxylases (PHs), alkene monooxygenases (AMOs), hyperthermophilic toluene monooxygenases (SsoMOs), and tetrahydrofuran/propane monooxygenases (THMOs). BMMs are unique among diiron proteins for their ability to hydroxylate a variety of hydrocarbon substrates including alkanes, alkenes, and aromatics.[3,4] Members of the sMMO and THMO subfamily are adept at converting small alkanes to their respective alcohols, whereas TMOs, PHs, and SsoMOs specialize in the regiospecific hydroxylation of aromatics. Although sMMOs can hydroxylate over 50 different compounds including aromatics,[1,5] most of the other family members cannot act on alkanes despite the fact that these enzymes are predicted by sequence homology and spectroscopy to have very similar, if not identical, diiron active sites.[1] Moreover, of the enzymes described above, only sMMO is capable of activating the inert C−H bond of methane, which is one of the most difficult reactions to perform in nature. The transformations performed by BMMs have not only inspired synthetic chemists to mimic this powerful chemistry but have also enabled many others to use these enzymes and their bacterial hosts for bioremediation and industrial biosynthetic applications, because some transformations are highly enantio- and regiospecific.[5,6]

Historically, most biochemical, spectroscopic, and computational investigations of BMM chemistry have focused on the diiron center of sMMO to probe its C−H and $O_2$ bond activation mechanisms. Detailed studies of substrate activation at the dinuclear iron center reveal that many factors controlling sMMO chemistry, as well as that of related diiron enzymes, are determined by the protein architecture.[1] Differences in substrate specificity between BMM family members raise important questions with respect to the tuning of their dimetallic iron centers. One ultimate goal is to understand aspects of the diiron chemistry that control $O_2$ and substrate reactivity and dictate a specific catalytic outcome. The present Account details progress made toward this objective from a structural perspective.

## Properties of Multicomponent Monooxygenases

Most BMMs, including the sMMO and PH subfamilies, require only three protein components for catalysis: a 200−255 kDa hydroxylase of the form $\alpha_2\beta_2\gamma_2$ that harbors the carboxylate-bridged diiron center, a 10−16 kDa cofactorless regulatory protein that couples ET with hydrocarbon substrate activation, and a 38−40 kDa [2Fe−2S]- and FAD-containing reductase that shuttles electrons from

Matthew H. Sazinsky received a B.S. in chemistry from Haverford College in 1995 and conducted his graduate work on multicomponent monooxygenases at MIT under the guidance of Stephen J. Lippard. At present, he is an NRSA postdoctorial fellow at Northwestern University investigating copper homeostasis in the lab of Amy Rosenzweig.

Stephen J. Lippard is the Arthur Amos Noyes Professor of Chemistry at MIT. His research focuses on bioinorganic chemistry including bacterial multicomponent monooxygenases, platinum anticancer drugs, and fluorescent probes for zinc and nitric oxide in the brain.

* To whom correspondence should be addressed. E-mail: lippard@mit.edu.



10.1021/ar030204v CCC: $33.50 
Published on Web 07/12/2006

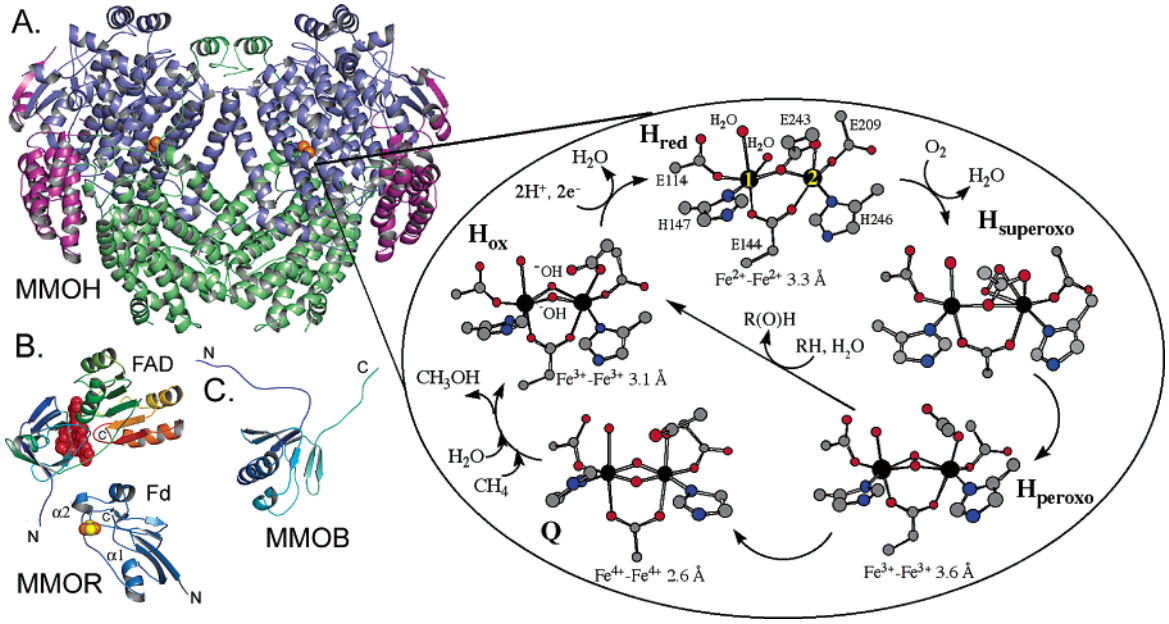


**FIGURE 1.** Structures of sMMO components and proposed reaction cycle. (A) MMOH; (B) the MMOR FAD and ferredoxin (Fd) domains; (C) MMOB. The MMOH α, $\beta$ and $\gamma$ subunits are colored blue, green, and purple, respectively. Iron, sulfur, and FAD are colored orange, yellow, and red, respectively, and are depicted as spheres. The sMMO reaction cycle is shown on the right with atoms colored according to type [iron (black), carbon gray), oxygen (red) and nitrogen (blue)].

NADH to the diiron center (Figure 1).[1] TMOs and SsoMOs utilize a 10−12 kDa Rieske protein as a fourth component that mediates ET from the reductase to the diiron center.[1,3] AMOs and THMOs are similar to the three-component sMMO and PH families, except that their hydroxylases do not have a $\gamma$ subunit.[3] The identity between the α subunits of the different subfamilies, where the diiron center is housed and hydroxylation chemistry takes place, ranges between 20 and 45%.[3]

**The Hydroxylase Component.** X-ray crystal structures of the methane and toluene/*o*-xylene monooxygenase hydroxylases (MMOH, Figure 1, and ToMOH) reveal a similar global topology, which may be characteristic of other BMM family members.[1,7,8] This component comprises two $\alpha\beta\gamma$ protomers, related by a 2-fold symmetry axis, that use protein−protein contacts between each of the α and $\beta$ subunits to form an $\alpha_2\beta_2\gamma_2$ heterodimer. The interface between the protomers forms a large canyon in the middle of the protein, which is proposed to be the docking site for binding the reductase, Rieske, and regulatory protein components.[1] The diiron center is housed within a four-helix bundle assembled by helices B, C, E, and F of the α subunit. Two of these helices, E and F, are on the hydroxylase surface and form a ridge of the canyon; the diiron center lies ∼12 Å beneath this ridge of the protein.

**The Diiron Center.** Among all known BMMs, a universally conserved set of glutamate and histidine ligands are responsible for binding the two iron atoms.[1] In the resting, diiron(III) state of $MMOH_{ox}$, one side of the dimetallic unit is formed by two histidine residues, which coordinate to positions distal to the active-site pocket, and a bridging carboxylate ion (Figures 1 and 2A). This three amino acid structural motif is conserved among $\Delta^9$ desaturase, RNR-R2, rubrerythrin, hemerythrin, ferritin, and bacterioferritin (Figure 2).[2] The remaining ligands in the primary coordination sphere of MMOH and ToMOH differ significantly from the those in the related diiron proteins in both identity and orientation. For MMOH and ToMOH, Fe1 is coordinated by a monodentate glutamate and a terminal water molecule, which hydrogen bonds to the dangling oxygen atom of the glutamate. Two monodentate carboxylates coordinate to Fe2. In the resting state, hydroxide ions occupy additional bridging positions to complete a pseudooctahedral geometry about the iron atoms, which are separated by 3.0−3.1 Å.[8] In different structures of MMOH and ToMOH, product alcohols and monoanions such as formate, acetate, and thioglycolate occupy the bridging position facing the hydrophobic active-site pocket, strongly implicating both C−H and $O_2$ activation at this site (parts A and B of Figure 2).[7−9]

For the diiron active sites of RNR-R2, $\Delta^9$ desaturase, bacterioferritin, and rubrerythrin, the flanking carboxylate ligands adopt different orientations and coordination modes, suggesting one way in which the chemistry of these enzymes is differentially tuned (Figure 2). In one structure of class 1c RNR-R2 from *Chlamydia trachomatis*, the coordinating ligands and geometric configuration at the diiron center are identical to those of $MMOH_{ox}$.[10] Unlike MMOH, however, the dinuclear iron center in this enzyme presumably generates an $Fe^{III}Fe^{IV}$ intermediate that performs the radical-forming function of the protein. Despite having nearly isostructural oxidized diiron(III) centers, the differences in catalytic function between MMOH and class 1c RNR-R2 emphasize the importance of the surrounding protein environment in controlling reactivity.

Upon two-electron reduction of MMOH to the diiron(II) form, mediated by the reductase component,

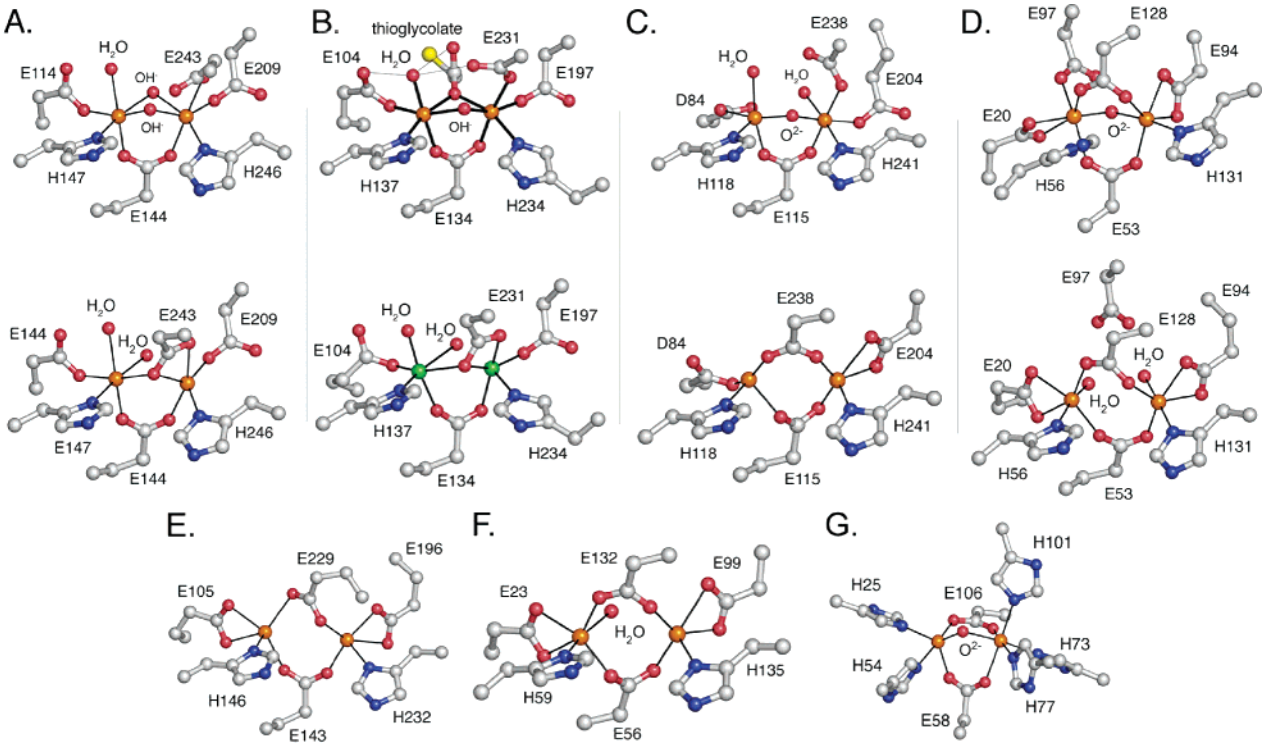


**FIGURE 2.** Dioxygen-utilizing carboxylate-bridged diiron centers. (A) Oxidized (top) and reduced (bottom) MMOH. (B) Oxidized (top) and $Mn^{II}$-reconstituted ToMOH (bottom). (C) Oxidized (top) and reduced (bottom) RNR-R2. (D) Oxidized (top) and reduced (bottom) rubrerythrin. (E) Reduced stearoyl-ACP $\Delta^9$ desaturase. (F) Reduced bacterioferritin. (G) Methemerythrin. The active site of *C. trachomatis* RNR-R2 is identical to that of $MMOH_{ox}$, although the bridging species is unknown. Fe1 is on the left, and Fe2 is on the right. All atoms and side chains are depicted in a ball and stick model and are colored by atom type [carbon (gray), oxygen (red), nitrogen (blue), sulfur (yellow), iron (orange), and manganese (green)].

MMOR, the bridging hydroxides are extruded, presumably as water molecules, and Glu-243 undergoes a carboxylate shift to occupy the bridging position cis to the histidine ligands while remaining chelated to Fe2 (Figures 1 and 2A).[1] A newly supplied water molecule coordinates weakly to Fe1 in a terminal position. As a consequence, the Fe−Fe distance increases to 3.3 Å and an open coordination site is formed on Fe2 facing the active-site pocket. X-ray absorption spectroscopy (XAS) and X-ray crystallographic investigations of the $Fe^{2+}$ and $Mn^{2+}$ forms of ToMOH, respectively, reveal that the reduced form of ToMOH is very similar to that of $MMOH_{red}$, except that the metal−metal distance for $ToMOH_{red}$ is slightly longer at 3.4 Å.[11,12] Density functional theory (DFT) calculations suggest that an open coordination position at Fe2 in MMOH is the primary site of $O_2$ activation by sMMO and perhaps all BMMs.[13] Synthetic model studies of carboxylate-rich diiron compounds also reveal the necessity of such open positions for oxygenation chemistry to occur.[14]

Glu-243 of MMOH is the only iron-coordinated amino acid that appears to alter its coordination mode and positioning as MMOH cycles through different oxidation states of the reaction cycle, according to both structural and computational investigations (Figure 1).[1,13,17] For RNR-R2, more than one iron-coordinating carboxylate alters its conformation, in addition to the residue analogous to Glu-243 (Figure 2). The carboxylate groups of Asp-84 and Glu-204 in RNR-R2 shift between monodentate and bidentate coordination modes to Fe1 and Fe2.[15] For rubrerythrin, the iron atom, Fe1, moves 1.8 Å to bind to either His-56 or Glu-97 when the oxidation state changes. The ligand positions remain fixed.[16] Unlike the situation in these enzymes, the positions of the analogous ligands and iron atoms in MMOH and ToMOH are restricted by second-sphere hydrogen-bonding interactions. Although different for MMOH than for ToMOH,[7] these restraints are presumably required to preserve conformational rigidity for these residues within the active site. For example, DFT calculations revealed that, without such a constraint, a monodentate terminal glutamate residue in reduced MMOH prefers to become bidentate and chelating, thus blocking a key coordination site required for $O_2$ activation.[17] The relative flexibility and positioning of carboxylate ligands in these different diiron proteins appear to be key components in tuning the reactivity of their respective dimetallic cores.

Helix E of the MMOH and ToMOH four-helix bundle has a $\pi$-helical segment in a region of the protein that contributes a glutamate ligand to the diiron center and several residues to the active-site pocket. This 10 amino acid stretch of $\pi$ helix in the middle of a mostly α-helical segment also occurs in RNR-R2, $\Delta^9$ desaturase, and rubrerythrin; it is absent in ferritin, bacterioferritin, and hemerythrin. The differences in helical structure may be of functional significance, but there is currently no clear understanding of such. The enzymes harboring the $\pi$-helical segment tend to have highly flexible iron ligands, which change position and orientation with metal oxida-

tion states, and variable Fe−Fe distances that presumably fluctuate throughout the catalytic cycle. The structures of MMOH with bound 6-bromohexan-1-ol and class 1b RNR-R2 from *Salmonella typhimurium* and *Mycobacterium tuberculosis* exhibit conformational changes in this helix.[9,18,19] For MMOH, residues 212−216 rearrange to be incorporated into the $\pi$-helical fold (Figure 3), whereas for RNR-R2, rearrangements in residues analogous to those in MMOH appear to facilitate greater solvent access to the diiron center. The helical change in sMMO increases the volume of the substrate cavity without altering the structure of the diiron center or allowing for greater solvent access through helices E and F. These structural observations suggest that the architecture of helix E serves an important, currently undefined, function in these enzymes. For bacterioferritin, ferritin, and hemerythrin, the purely α-helical nature of the four-helix bundle may reflect greater rigidity and less dependence on conformational changes for function.

**Conserved Active-Site Asparagine and Threonine Residues.** The iron-coordinating ligands are not the only residues that undergo redox-dependent conformational changes. Asn-214 of MMOH, a highly conserved residue on helix E, sits 4.0 Å above Glu-243 on the α-subunit surface in a gap formed at the interface of helices E and F. Reduction of the protein to either the $Fe^{II}Fe^{III}$ or $Fe^{II}Fe^{II}$ form induces the Asn-214 side chain to shift inward, toward the diiron center (Figure 3).[8] Identical motions are observed in the oxidized versus the $Mn^{II}$-reconstituted forms of ToMOH.[7,11] Thr-213 is also a highly conserved residue, the side chain of which adopts alternate rotameric conformations in the active site of MMOH. Although these changes do not always appear to be redox-dependent, in most of the oxidized structures of MMOH, the threonine hydroxyl group points toward the back of the hydrophobic substrate pocket, whereas in reduced MMOH, it points toward the diiron center.[8] In the 6-bromohexanol-soaked structure of MMOH with more $\pi$-helical character in the E helix, Thr-213 and Asn-214 are repositioned to lie exclusively on the MMOH surface (Figure 3). The functional significance of this reorientation is unclear. Except for $\Delta^9$ desaturase, which is the only other diiron protein having a similarly positioned threonine in the active site, the use of these two residues in diiron proteins is unique to BMMs.

The crystal structures of oxidized and reduced MMOH exhibit several different solvent configurations in the active site involving hydrogen bonding to the terminal water on Fe1, Glu-243, Asn-214, and Thr-213. On the basis of these observations, it was proposed that Thr-213 and Asn-214 may participate in proton-transfer events.[8] Mutating the analogous threonine in toluene 4-monooxygenase (T4MO) did not significantly affect the turnover rate or the coupling of NADH consumption to product formation, suggesting that it is not critical for catalysis.[20] Mutagenesis of Asn-202 in ToMOH, on the other hand, revealed this residue to be vital for the binding of the regulatory protein, ToMOD.[21] The exact functions of the

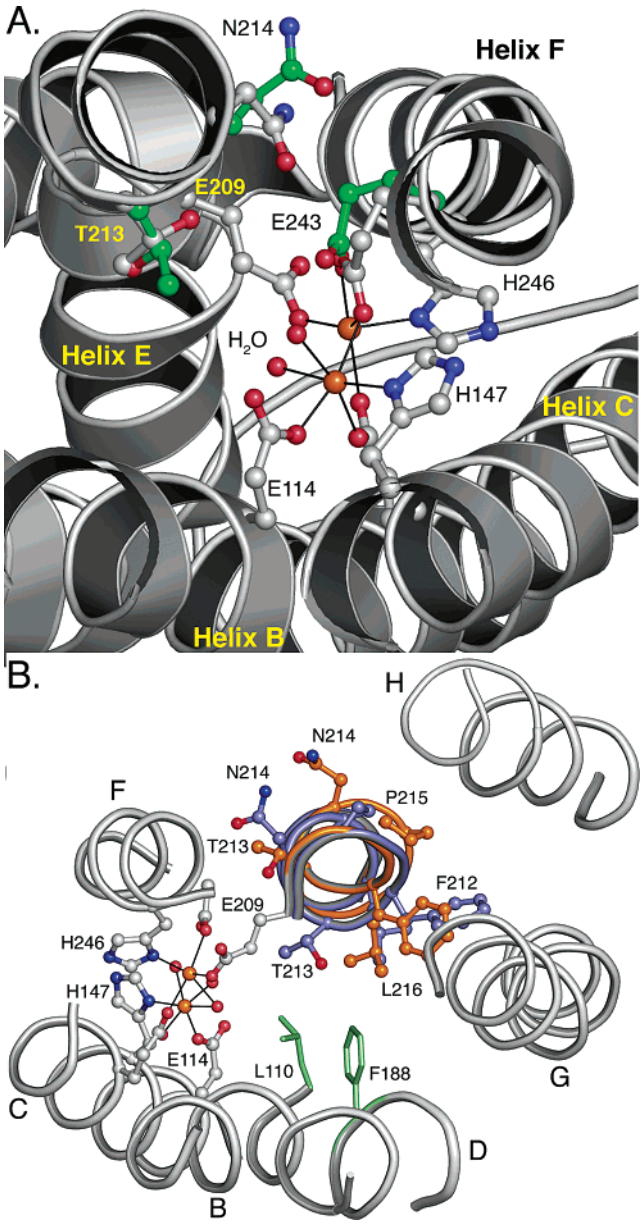


**FIGURE 3.** Structural changes in the MMOH active site. (A) Alternate conformations of Thr-213, Asn-214, and Glu-243 in the oxidized (green) and reduced (gray) forms of MMOH. Glu-243 resides ∼4.0 Å underneath Asn-214. Hydrogen bonding between bound solvent and Asn-214, Glu-243, and Thr-213 and the terminal water on Fe1 varies from structure to structure and is therefore not depicted. (B) Conformational changes in residues 212−216 of helix E. The typical oxidized configuration is colored blue, while the 6-bromohexanol-altered structure is depicted in orange. Helices A−H are represented as gray ribbons. Leu-110 and Phe-188 (green) represent the back of the active-site pocket.

universally conserved threonine and asparagine are poorly understood and warrant future investigation.

**Hydrogen-Bonding Networks.** As stated above, some residues in the second and third coordination spheres around the diiron center provide conformational constraints that control the geometry of the diiron center. One hydrogen-bonding network in particular extends ∼12−13 Å from iron-coordinating histidines through the four-helix bundle to the hydroxylase surface in the canyon

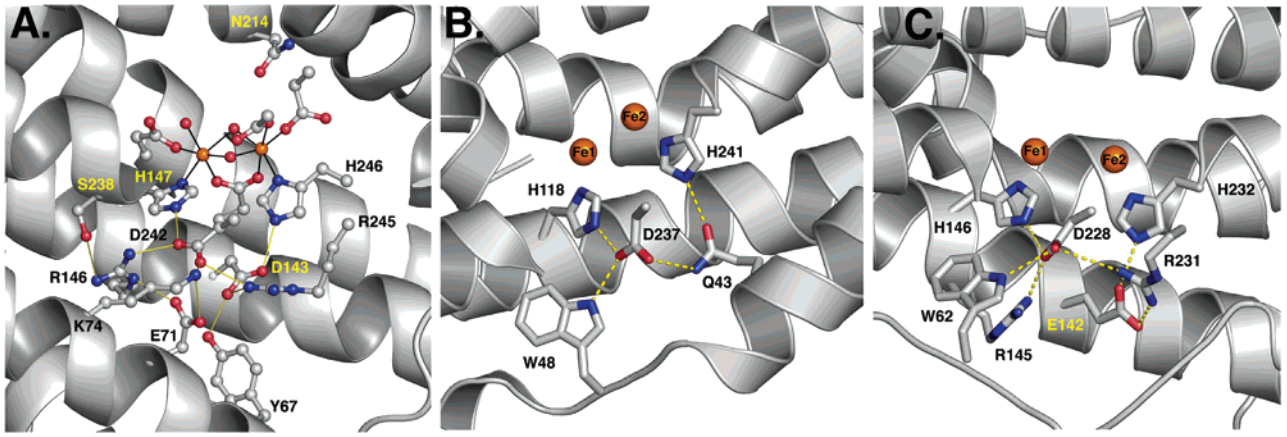


**FIGURE 4.** Hydrogen-bonding network behind the diiron centers of (A) MMOH, (B) RNR-R2, and (C) stearoyl-ACP $\Delta^9$ desaturase.

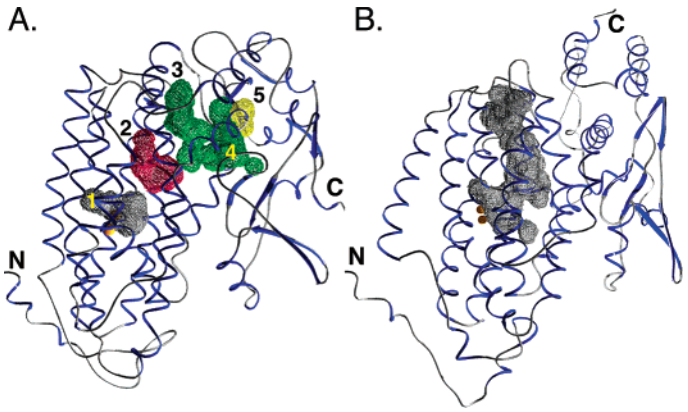


**FIGURE 5.** Cavities and channels in the α subunit of (A) MMOH and (B) ToMOH. The irons are depicted as yellow spheres, and cavities 1−5 in MMOH are labeled accordingly. Cavities 3 and 4 (green) in MMOH are connected.

region at helix A (Figure 4). In all BMMs, the residues contributing to this network are absolutely conserved, implicating this region as essential for either the folding of α subunit or ET. Analogous networks in RNR-R2, $\Delta^9$ desaturase, rubrerythrin, and bacterioferritin involve similar residues.[2] In RNR-R2, a conserved tryptophan in the pathway forms a transient radical intermediate that is required for generating the catalytic $Fe^{III}Fe^{IV}$ intermediate and the tyrosyl radical,[15] demonstrating how the second and third coordination shells of a diiron enzyme can assist in catalytic function (Figure 4B). The hydrogen bonding in RNR-R2 is most similar to that in $\Delta^9$ desaturase, although no radical has been observed in this enzyme (Figure 4C).

**Access to the Diiron Center.** Crystallographic investigations into substrate and product binding reveal the presence of cavities and channels in the α subunit of BMMs that may function to orchestrate the movements of small molecules for efficient catalysis.[7,9] The MMOH α subunit contains five major hydrophobic cavities, three of which lead from the active-site pocket, cavity 1, to the protein surface.[1] A larger channel has been identified in ToMOH (Figure 5).[7] Crystal structures of MMOH and ToMOH with product and substrate analogues bound to these regions of the α subunit have provided strong evidence that these cavities and channels are a primary pathway by which small molecules access the diiron center.[7,9] The major structural difference between MMOH and ToMOH is that the diiron center of the former appears more protected from the bulk solvent, owing to amino acids that gate access between the different cavities. These gating residues, however, can alter their conformations to allow for small molecule translocation between cavities.[9] Hydrophobic cavities may be required for sequestering gaseous substrates such as methane, whereas a larger channel may be better suited for efficient movement of aromatic compounds to and from the diiron center. Although sMMOs can hydroxylate aromatics, TMOs and PHs are 20 times more efficient at performing this reaction,[5,22] perhaps because of easier substrate access and/or product egress.

An alternate entrance to the diiron center may be directly through helices E and F of the four-helix bundle. Surface calculations show that only a single residue, Asn-214 (Asn-202 in ToMOH), blocks access to the diiron center. In $MMOH_{red}$, the positional change in Asn-214 results in the formation of a large crevice on the surface of the protein between helices E and F that extends toward the active site and in one protomer forms a pore connecting the surface to the diiron center.[8,9] These redox-dependent changes suggest that the residue may control the passage of small species such as $CH_4$, $CH_3OH$, $H_2O$, $H_3O^+$, and $O_2$ to and from the active site.

The homologous diiron enzymes in the superfamily employ their own specific schemes by which to accommodate small molecule binding and extrude solvent. RNR-R2, hemerythrin, and rubrerythrin have small hydrophobic active-site pockets specific for $O_2$ and $O_2$-derived substrates.[2] $\Delta^9$ desaturase, like ToMOH, has a long hydrophobic channel required to accommodate its fatty acid substrate.[2] The different architectural schemes employed for substrate access undoubtedly correlate to the specific function of the protein.

## Component Interactions and Structural Affects

Efficient hydroxylation of substrates by BMMs is not possible without the reductase and regulatory proteins, both of which exert profound structural and spectroscopic

effects on the hydroxylase and help to promote substrate activation at the diiron center. One of the biggest challenges to understanding the mechanism of hydrocarbon oxidation by BMMs is correlating the interactions between the component complexes with the chemical and structural changes at or near the diiron center.

**Reductase Binding and the ET Pathway.** NMR structures of the individual ferredoxin and FAD domains of the sMMO reductase, MMOR, have been determined (Figure 1),[23] but the geometry of the full-length protein revealing the packing of the two domains against one another is currently unknown. For this class of reductase, electrons are shuttled sequentially from NADH through the flavin and [2Fe−2S] cofactors to the diiron center of the hydroxylase.

Initial chemical cross-linking studies indicated that *M. trichosporium* MMOR interacts exclusively with the MMOH $\beta$ subunit.[24] More recent chemical cross-linking work using either *M. capsulatus* MMOR or its ferredoxin domain ($MMOR_{Fd}$) suggests that they primarily interact with the MMOH α subunit.[25] NMR line-broadening experiments on $MMOR_{Fd}$ in the presence of MMOH indicate that amino acids located on the face of the protein containing the [2Fe−2S] cluster and helices $\alpha_1$ and $\alpha_2$ pack against the hydroxylase surface (Figure 1).[26] The MMOR FAD domain does not form cross-links to MMOH, but small differences in the binding affinities of MMOR (0.4 $\mu$M) and $MMOR_{Fd}$ (0.6 $\mu$M) for MMOH imply that regions of the FAD domain may be involved in interactions with the hydroxylase.[25,27]

Application of the Marcus theory to intermolecular ET events between MMOR and MMOH indicate that the [2Fe−2S] cluster of the former may lie ∼11−14 Å from the dinuclear iron center of MMOH.[27] Using the 11−14 Å distance, NMR line-broadening data, and electrostatic surface and shape complementarity, computational modeling places the $MMOR_{Fd}$ docking site on the α subunit near the hydrogen-bonding network behind the iron-coordinating histidines that lead to the canyon surface (Figure 6). The docking site positions the ferredoxin domain near the $\beta$-subunit N terminus and may explain previously observed cross-linking data. This speculative binding site outlines a putative ET pathway between the metal centers in MMOR and MMOH. For a comparison, the $\{Fe(SCys)_4\}$ site of rubrerythrin and the cytochrome in bacterioferritin are both within 14 Å of their respective diiron centers, near similar hydrogen-bonding networks positioned behind their iron-coordinating histidines.[2] More recently, the $\Delta^9$-desaturase ferredoxin protein was proposed to bind near an analogous network.[28]

**ET.** In the sMMO system, both the regulatory (MMOB) and reductase proteins alter the redox potentials of MMOH.[1,29,30] MMOB decreases the potentials of the diiron center by ∼100−200 mV, making it harder to reduce, whereas MMOR restores the potentials to slightly above the level observed before MMOB binding, which favors reduction. The equilibrated MMOH−MMOB−MMOR complex, when reduced with NADH, has relatively fast intermolecular ET rates compared to those of the preformed

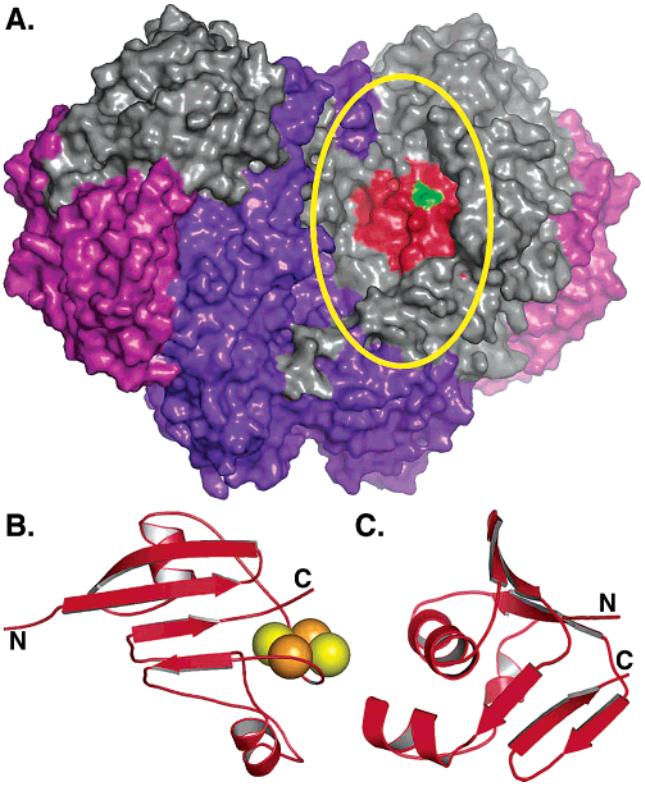


**FIGURE 6.** Docking models of the sMMO component complexes. (A) Predicted $MMOR_{Fd}$ and MMOB binding area (yellow ellipse) on the MMOH surface. The axes of the ellipse were chosen to encompass the shapes of the $MMOR_{Fd}$ and MMOB components when placed next to one another. The α-, $\beta$-, and $\gamma$-subunit surfaces are colored gray, purple, and violet, respectively. MMOH surfaces within 14 Å of the diiron center, the likely position of the MMOR [2Fe−2S] cluster, are colored in red. Asn-214 is colored green. (B) $MMOR_{Fd}$ and (C) MMOB, oriented so as to place the face packing against the hydroxylase surface pointing into the paper. The [2Fe−2S] center is represented by orange and yellow spheres.

MMOH−MMOB complex with three-electron-reduced MMOR, which are more than twice as slow.[30] Moreover, ET between chemically reduced MMOR and MMOH is 4-fold faster without MMOB.[30] On the basis of these findings, it is postulated that MMOB and MMOR partition intermolecular ET into slow and fast pathways, respectively.[30] The differences indicate that MMOB influences the structure of MMOH and that MMOR perturbs the structures of both MMOH and the MMOH−MMOB complex. Despite alterations in the redox potentials of MMOH, MMOR does not significantly affect the spectroscopic properties of the hydroxylase diiron center, whereas MMOB does (see below).[1] Coupling of NADH consumption to substrate hydroxylation is most efficient when the regulatory protein is present, suggesting that it is required somehow for ET.[29,30] It must be noted, however, that MMOH and MMOB do not alter the redox potentials of the MMOR cofactors,[1,30] that neither MMOB nor MMOR competes for the same binding site on the hydroxylase surface nor interacts with the other in solution,[29] and that MMOB and MMOR do not interact with each other when bound to MMOH.[31] The available findings to date indicate that a dynamic relationship exists between the three

sMMO components, but at this stage, relatively little is known about how they work in concert to facilitate ET.

**Structural Effects of the Regulatory Protein.** Every known BMM requires a small regulatory protein for efficient catalysis that increases the reactivity of the hydroxylase by 30−150-fold (Figure 1).[3,22,24] This component may function to shift the relative population of hydroxylase molecules toward an active conformation at a specific step in the catalytic cycle (Figure 1), knowledge of which is essential to our fundamental understanding of the BMM function. Moreover, its role in activating the diiron center of BMMs is unique because no related diiron proteins in the superfamily require such a protein cofactor.

Early X-ray absorption spectroscopic work on sMMO revealed that MMOB has no remarkable affect on the spectra or fitting parameters, indicating that this protein does not significantly perturb the iron environment in either the oxidized or reduced states of the protein.[1] Recent advances in methodology have allowed for reinvestigation of this question by using better model compounds and computational simulations.[12] The addition of the regulatory protein to $MMOH_{red}$ and $ToMOH_{red}$ did not change the structure of the diiron center, but the Debye−Waller factors, which are a measure of thermal disorder for a fit atom, decreased. This finding indicated that binding of the regulatory protein to the hydroxylase may serve to limit the flexibility or motion of the metal-coordinating ligands.

Circular dichroism and magnetic circular dichroism spectroscopic studies of $MMOH_{red}$ indicate that MMOB alters the ligand field environment of only one of the iron atoms.[32] The other iron atom is perturbed by substrates and inhibitors but only when MMOB is bound to the hydroxylase. Comparisons between the different crystal structures of MMOH in its various oxidation states and metal-reconstituted forms indicate that the position of Fe2 and its ligands vary the most from structure to structure, whereas Fe1 and its ligands do not move.[8,33] On the basis of this analysis, it was hypothesized that Fe2, the iron closest to the canyon surface, is most likely perturbed by MMOB, whereas Fe1 associates more readily with bound small molecules.[8,33] The variable positioning of the bound water molecule facing the active-site pocket, which shifts between bridging, semi-bridging, and terminal coordination in these different reduced structures of MMOH, suggested that MMOB may facilitate the displacement of this water so that $O_2$ can react more readily with the diiron center.[33,34]

$MMOH_{ox}$ has two high-spin $Fe^{III}$ ions that are antiferromagnetically coupled to form an electron paramagnetic resonance (EPR) silent, diamagnetic diiron(III) center. Cryoreduction of the diferric center by $\gamma$-irridation at 77 K produces an EPR-active mixed-valent $Fe^{III}Fe^{II}$ dimetallic center with an $S = {}^1/_2$ spin state that maintains the structure of $MMOH_{ox}$. Such cryo-reduced samples have facilitated investigations of the physiologically relevant oxidized form of MMOH vis-à-vis that of the mixed-valent state, which is not a true intermediate based on our current understanding.[1] EPR spectroscopy indicates that MMOB has no measurable affect on the $\gamma$-irradiated diiron(III) form of MMOH. When $MMOH_{ox}$ is complexed to products such as methanol and phenol, spectral changes are observed upon addition of MMOB.[35] Interestingly, the binding of glycerol and DMSO to $MMOH_{ox}$ is favored only in the presence of MMOB. These findings suggested that MMOB may participate in modulating substrate entrance or product release.

More recent biochemical investigations support the postulated role for MMOB in controlling access to the active site. An MMOB quadruple mutant, in which residues predicted to interact with the hydroxylase surface were changed to alanine, allowed for enhanced reactivity of larger substrates such as furan and nitrobenzene with intermediate Q, suggesting that MMOB acts as a molecular sieve that guards the substrate and solvent entrance.[36] Metal reconstitution experiments in which MMOB binding was observed to retard iron addition to and removal from MMOH also imply that the regulatory protein can limit solvent access, either by occluding access to the active-site pocket or rigidifying this region of MMOH.[33] At present, it is unknown whether the regulatory proteins in the other BMM systems exert similar substrate-gating effects.

In addition to its role in governing small molecule access to the diiron center, the regulatory protein alters the regiospecificity of the hydroxylase-catalyzed reaction.[37,38] In the sMMO system from *Methylosinus trichosporium* OB3b without MMOB, secondary alcohols and *m*-nitrophenol are the preferred products of alkane and nitrobenzene hydroxylation, respectively.[37] The addition of MMOB shifts the product ratios such that mostly primary alcohols and *p*-nitrophenol are formed. Similar changes in product regiospecifity are observed in the T4MO system, where, upon the addition of the regulatory protein, the yield of *p*-cresol formation shifts from 69 to 96%.[6] To exert such regiospecific changes in BMMs, the regulatory protein must alter the structure of the active-site pocket. Mutagenesis studies on T4MOH in combination with product analysis using toluene and alternative aromatic compounds as substrates indicate that residues near the universally conserved active-site threonine, which resides on helix E, are perturbed by the regulatory protein.[6,20] This finding was the first to suggest exactly where the regulatory protein may influence the structure of a hydroxylase and is consistent with the Asn-202 mutagenesis data placing ToMOD binding here.[21] Moreover, the α-to-$\pi$-helix change in the 6-bromohexan-1-ol-bound structure of MMOH suggests how the effector protein may alter this region of the hydroxylase to influence the product distributions (Figure 3B). For example, when Thr-213 is rotated out of the active-site pocket, the increase in cavity volume may provide more room for hydroxylation at the primary carbon of alkanes and favor *p*-nitrophenol formation.

**Regulatory Protein Docking and Diiron Center Tuning.** From a variety of data, a picture has begun to emerge for the binding of the regulatory protein on the surface

of the hydroxylase. Chemical cross-linking,[24] mass spectrometry,[39] mutagenesis,[21] and metal reconstitution experiments[33] clearly indicate that this protein binds at helices E and F of the four-helix bundle in the canyon region of the hydroxylase, a position consistent with the various spectroscopic, redox, and regiospecificity changes described above. From this information, we have constructed an MMOH−MMOB docking model, which places several conserved residues that experience greater than average NMR line broadening in the presence of MMOH[31] at the protein−protein interface such that the electrostatic surfaces between these proteins are complemented (Figure 6). A recently determined crystal structure of a complex between the hydroxylase and effector protein of PH[40] places the latter over helices E and F in the canyon and is consistent with the aforementioned observations for sMMO. On the basis of the sMMO docking model and the phenol hydroxylase structure, it is possible to see how MMOB may gate substrate (or solvent) access to the active site, possibly through the four-helix bundle, and serve to rigidify the region around the diiron center. Given the findings described above, we predict that the dinuclear iron center of MMOH may not be significantly altered when the regulatory protein is bound, whereas the configuration of the active-site pocket, possibly owing to an α-to-$\pi$-helix transition in helix E, most likely is affected. We further speculate that different BMM systems may use their effector protein for slightly different purposes. MMOB requires a flexible 35 amino acid N terminus to induce structural and redox changes in MMOH, whereas the TMO and PH proteins do not.[1] Additional high-resolution crystal structures of protein component complexes in different oxidation states will allow us to evaluate further the relationships between structure and function in the BMM family of enzymes.

**Why Methane?** The most extensively studied BMM mechanism is that of sMMO, where the (peroxo)diiron(III)($H_{peroxo}$) and di($\mu$-oxo)diiron(IV) (Q) intermediates effect substrate epoxidation and hydroxylation (Figure 1).[1,41] Given the similarity between the diiron centers of MMOH and ToMOH, we speculate that both enzymes traverse similar intermediates, at least at the (peroxo)diiron(III) level. Recent spectroscopic evidence indicates that ToMOH and PH-H may form a peroxo intermediate that is structurally different from that of MMOH.[1,13,42,43] Moreover, ToMOH and PH-H fail to generate intermediate Q, which has a short Fe−Fe distance of 2.5 Å. The inability of TMO and PH to hydroxylate methane and other alkanes may be due to these differences in the peroxo intermediate and perhaps the inability of these enzymes to compress the Fe−Fe center sufficiently to generate Q.

The fate of the peroxo intermediate may also depend on the surrounding protein environment. Differences in solvent and substrate accessibility, such as cavities in MMOH versus channels in ToMOH (Figure 5), and structural changes imposed by the effector protein in each BMM system may have a significant influence on substrate reactivity. For the TMO and PH systems, methane may simply be too small of a substrate to block adequately solvent access from the channel. Aromatic substrates, on the other hand, may serve as convenient steric impediments that limit undesired solvent penetration into the active site along this route. Modulating the size and morphology of the active-site pocket as well as the modes of entrance to the diiron center may therefore be nature's mechanism for governing substrate reactivity and regiospecificity.

## Outlook

The fundamental properties that differentiate carboxylate-bridged diiron proteins from one another remain to be clarified, and the comparisons presented here offer avenues for future investigation. Further clues toward understanding fully the BMM chemistry will be revealed once we have knowledge about the structural changes induced by component interactions. One of the major challenges in elucidating the mechanism of hydrocarbon oxidation in BMMs is to correlate the structure of the component complexes with the movements of the amino acids at the active site at each stage of the reaction cycle. The redox-dependent and component-induced conformational changes known to date suggest that the hydroxylase structure, even beyond the diiron center, is in flux throughout the catalytic cycle. The substrate specificity and reactivity exhibited by the BMM subfamily members may be attributed to important alterations in the iron coordination sphere and active-site pocket residues, the nature of which is slowly becoming apparent.

## References

(1) Merkx, M.; Kopp, D. A.; Sazinsky, M. H.; Blazyk, J. L.; Müller, J.; Lippard, S. J. Dioxygen activation and methane hydroxylation by soluble methane monooxygenase: A tale of two irons and three proteins, *Angew. Chem., Int. Ed.* **2001**, *40*, 2783−2807 and references therein.

(2) Kurtz, D. M., Jr. Structural similarity and functional diversity in diiron-oxo proteins, *J. Biol. Inorg. Chem.* **1997**, *2*, 159−167 and references therein.

(3) Notomista, E.; Lahm, A.; Di Donato, A.; Tramontano, A. Evolution of bacterial and archaeal multicomponent monooxygenases, *J. Mol. Evol.* **2003**, *56*, 435−445.

(4) Leahy, J. G.; Batchelor, P. J.; Morcomb, S. M. Evolution of the soluble diiron monooxygenases, *FEMS Microbiol. Rev.* **2003**, *27*, 449−479.

(5) Colby, J.; Stirling, D. I.; Dalton, H. The soluble mono-oxygenase of *Methylococcus capsulatus* (Bath). Its ability to oxygenate *n*-alkanes, ethers, and alicyclic, aromatic and heterocyclic compounds, *Biochem. J.* **1977**, *165*, 395−402.

(6) Mitchell, K. H.; Studts, J. M.; Fox, B. G. Combined participation of hydroxylase active residues and effector protein binding in a *para* to *ortho* modulation of toluene 4-monooxygenase regiospecificity, *Biochemistry* **2002**, *41*, 3176−3188.

(7) Sazinsky, M. H.; Bard, J.; Di Donato, A.; Lippard, S. J. Structure of the toluene/*o*-xylene monooxygenase hydroxylase from *Pseudomonas stutzeri* OX1: Substrate channeling and active site tuning of multicomponent monooxygenases, *J. Biol. Chem.* **2004**, *279*, 30600−30610.

(8) Whittington, D. A.; Lippard, S. J. Crystal structures of the soluble methane monooxygenase hydroxylase from *Methylococcus capsulatus* (Bath) demonstrating geometrical variability at the dinuclear iron active site, *J. Am. Chem. Soc.* **2001**, *123*, 827−838 and references therein.

(9) Sazinsky, M. H.; Lippard, S. J. Product bound structures of the soluble methane monooxygenase hydroxylase from *Methylococcus capsulatus* (Bath): Protein motion in the α-subunit, *J. Am. Chem. Soc.* **2005**, *127*, 5814−5825.

(10) Högbom, M.; Stenmark, P.; Voevodskaya, N.; McClarty, G.; Gräslund, A.; Nordlund, P. The radical site chlamydial ribonucleotide reductase defines a new R2 subclass, *Science* **2004**, *305*, 245−248.
(11) McCormick, M. S.; Sazinsky, M. H.; Condon, K. L.; Lippard, S. J. Manuscript submitted for publication.
(12) Jackson Rudd, D.; Sazinsky, M. H.; Lippard, S. J.; Hedman, B.; Hodgson, K. O. X-ray absorption spectroscopic study of the reduced hydroxylases of methane monooxygenase and toluene/*o*-xylene monooxygenase: Differences in active site structure and effects of the coupling proteins MMOB and ToMOD, *Inorg. Chem.* **2005**, *44*, 4546−4554.
(13) Baik, M.-H.; Newcomb, M.; Friesner, R. A.; Lippard, S. J. Mechanistic studies on the hydroxylation of methane by methane monooxygenase, *Chem. Rev.* **2003**, *103*, 2385−2420.
(14) Yoon, S.; Lippard, S. J. Water affects the stereochemistry and dioxygen reactivity of carboxylate-rich diiron(II) models for the diiron centers in dioxygen-dependent non-heme enzymes, *J. Am Chem. Soc.* **2005**, *127*, 8386−8397.
(15) Stubbe, J.; Nocera, D. G.; Yee, C. S.; Chang, M. C. Y. Radical initiation in the class I ribonucleotide reductase: Long-range proton-coupled electron transfer? *Chem. Rev.* **2003**, *103*, 2167−2202.
(16) Jin, S.; Kurtz, D. M., Jr.; Lui, Z., J.; Rose, J.; Wang, B. C. X-ray crystal structures of reduced rubrerythrin and its azide adduct: A structure-based mechanism for a non-heme diiron peroxidase, *J. Am Chem. Soc.* **2002**, *124*, 9845−9855.
(17) Dunietz, B. D.; Beachy, M. D.; Cao, Y.; Whittington, D. A.; Lippard, S. J.; Friesner, R. A. Large scale ab initio quantum chemical calculation of the intermediates in the soluble methane monooxygenase catalytic cycle, *J. Am Chem. Soc.* **2000**, *122*, 2828−2839.
(18) Eriksson, M.; Jordan, A.; Eklund, H. Structure of *Salmonella typhimurium* nrdF ribonucleotide reductase in its oxidized and reduced forms, *Biochemistry* **1998**, *37*, 13359−13369.
(19) Uppsten, M.; Davis, J.; Rubin, H.; Uhlin, U. Crystal structure of the biologically active form of class Ib ribonucleotide reductase small subunit from *Mycobacterium tuberculosis*, *FEBS Lett.* **2004**, *569*, 117−122.
(20) Pikus, J. D.; Mitchell, K. H.; Studts, J. M.; McClay, K.; Steffan, R. J.; Fox, B. G. Threonine 201 in the diiron enzyme toluene 4-monooxygenase is not required for catalysis, *Biochemistry* **2000**, *39*, 791−799.
(21) Cadieux, E.; Murray, L. J.; McCormick, M. S.; Sazinsky, M. H.; Lippard, S. J. Manuscript in preparation.
(22) Cadieux, E.; Vrajmasu, V.; Achim, C.; Powlowski, J.; Münck, E. Biochemical, Mössbauer, and EPR studies of the diiron dluster of phenol hydroxylase from *Pseudomonas* sp. strain CF600, *Biochemistry* **2002**, *41*, 10680−10691.
(23) Chatwood, L.; Müller, J.; Gross, J.; Wagner, G.; Lippard, S. J. NMR Structure of the flavin domain from soluble methane monooxygenase reductase from *Methylococcus capsulatus* (Bath), *Biochemistry* **2004**, *43*, 11983−11991.
(24) Fox, B. G.; Liu, Y.; Dege, J. E.; Lipscomb, J. D. Complex formation between the protein components of methane monooxygenase from *Methylosinus trichosporium* Ob3b: Identification of sites of component interaction, *J. Biol. Chem.* **1991**, *266*, 540−550.
(25) Kopp, D. A.; Berg, E. A.; Costello, C. E.; Lippard, S. J. Structural features of covalently cross-linked hydroxylase and reductase proteins of soluble methane monooxygenase as revealed by mass spectrometric analysis, *J. Biol. Chem.* **2003**, *278*, 20939−20945.
(26) Müller, J.; Lugovskoy, A. A.; Wagner, G.; Lippard, S. J. NMR structure of the [2Fe−2S] ferredoxin domain from soluble methane monooxygenase reductase and interaction with its hydroxylase, *Biochemistry* **2002**, *41*, 42−51.
(27) Blazyk, J. L.; Gassner, G. T.; Lippard, S. J. Intermolecular electron-transfer reactions in soluble methane monooxygenase: A role for hysteresis in protein function, *J. Am Chem. Soc.* **2005**, *127*, 17364−17376.
(28) Sobrado, P.; Lyle, K. S.; Kaul, S. P.; Turco, M. M.; Arabshahi, I.; Marwah, A.; Fox, B. G. Identification of the binding region of the [2Fe−2S] ferredoxin in stearoyl-acyl carrier protein desaturase: Insight into the catalytic complex and mechanism of action, *Biochemistry* **2006**, *45*, 4848−4858.
(29) Gassner, G. T.; Lippard, S. J. Component interactions in the soluble methane monooxygenase system from *Methylococcus capsulatus* (Bath), *Biochemistry* **1999**, *38*, 12768−12785.
(30) Blazyk, J. L.; Gassner, G. T.; Lippard, S. J. Intermolecular electron-transfer reactions in soluble methane monooxygenase: A role for hysteresis in protein function, *J. Am Chem. Soc.* **2005**, *127*, 17364−17376 and references therein.
(31) Walters, K. J.; Gassner, G. T.; Lippard, S. J.; Wagner, G. Structure of the soluble methane monooxygenase regulatory protein B, *Proc. Natl. Acad. Sci. U.S.A.* **1999**, *96*, 7877−7882.
(32) Pulver, S. C.; Froland, W. A.; Lipscomb, J. D.; Solomon, E. I. Ligand field circular dichroism and magnetic circular dichroism studies of component B and substrate binding to the hydroxylase component of methane monooxygenase, *J. Am. Chem. Soc.* **1997**, *119*, 387−395.
(33) Sazinsky, M. H.; Merkx, M.; Cadieux, E.; S., T.; Lippard, S. J. Preparation and X-ray structures of metal-free, dicobalt and dimanganese forms of soluble methane monooxygenase hydroxylase from *Methylococcus capsulatus* (Bath), *Biochemistry* **2004**, *43*, 16263−16276.
(34) Gherman, B. F.; Baik, M.-H.; Lippard, S. J.; Friesner, R. A. Dioxygen activation in methane monooxygenase: A theoretical study, *J. Am. Chem. Soc.* **2004**, *126*, 2978−2990.
(35) Davydov, R.; Valentine, A. M.; Komar-Panicucci, S.; Hoffman, B. M.; Lippard, S. J. An EPR study of the dinuclear iron site in the soluble methane monooxygenase from *Methylococcus capsulatus* (Bath) reduced by one electron at 77 K: The effects of component interactions and the binding of small molecules to the diiron(III) center, *Biochemistry* **1999**, *38*, 4188−4197.
(36) Wallar, B. J.; Lipscomb, J. D. Methane monooxygenase component B mutants alter the kinetic steps throughout the catalytic cycle, *J. Am. Chem. Soc.* **2001**, *40*, 2220−2233.
(37) Froland, W. A.; Andersson, K. K.; Lee, S. K.; Liu, Y.; Lipscomb, J. D. Methane monooxygenase component B and reductase alter the regioselectivity of the hydroxylase component-catalyzed reactions, *J. Biol. Chem.* **1992**, *267*, 17588−17597.
(38) Pikus, J. D.; Studts, J. M.; McClay, K.; Steffan, R. J.; Fox, B. G. Changes in the regiospecificity of aromatic hydroxylation produced by active site engineering in the diiron enzyme toluene 4-monooxygenase, *Biochemistry* **1997**, *36*, 9283−9289.
(39) Brazeau, B. J.; Wallar, B. J.; Lipscomb, J. D. Effector proteins from P450cam and methane monooxygenase: Lessons in tuning nature's powerful reagents, *Biochem. Biophys. Res. Comm.* **2003**, *312*, 143−148.
(40) Sazinsky, M. H.; Dunten, P.; McCormick, M. S.; Lippard, S. J. Manuscript in preparation.
(41) Beauvais, L. G.; Lippard, S. J. Reactions of the peroxo intermediate of soluble methane monooxygenase hydroxylase with ether, *J. Am. Chem. Soc.* **2005**, *127*, 7370−7378.
(42) Murray, L. J.; Serres-García, R.; Naik, S.; Huynh, B. H.; Lippard, S. J. Dioxygen activation at non-heme diiron centers: Characterization of intermediates in a mutant form of toluene/*o*-xylene monooxygenase hydroxylase, *J. Am. Chem. Soc.* **2006**, *128*, 7458−7459.
(43) Izzo, V.; Serres-García, R.; Naik, S.; Huynh, B. H.; Lippard, S. J. Unpublished results.

AR030204V